Technology in Cancer Research and Treatment
ISSN 1533-0346
Volume 10, Number 6, December 2011

Feasibility of Identification of Gamma Knife Planning Strategies by Identification of Pareto Optimal Gamma Knife Plans

Cole A. Giller, MD, PhD, MBA

Department of Neurosurgery,
Georgia Health Sciences University,
1120 15th Street, Augusta, GA 30912

www.tcrt.org

The use of conformity indices to optimize Gamma Knife planning is common, but does not address important tradeoffs between dose to tumor and normal tissue. Pareto analysis has been used for this purpose in other applications, but not for Gamma Knife (GK) planning. The goal of this work is to use computer models to show that Pareto analysis may be feasible for GK planning to identify dosimetric tradeoffs. We define a GK plan A to be *Pareto dominant* to B if the prescription isodose volume of A covers more tumor but not more normal tissue than B, or if A covers less normal tissue but not less tumor than B. A plan is *Pareto optimal* if it is not dominated by any other plan. Two different Pareto optimal plans represent different tradeoffs between dose to tumor and normal tissue, because neither plan dominates the other. 'GK simulator' software calculated dose distributions for GK plans, and was called repetitively by a genetic algorithm to calculate Pareto dominant plans. Three irregular tumor shapes were tested in 17 trials using various combinations of shots. The mean number of Pareto dominant plans/trial was 59 ± 17 (sd). Different planning strategies were identified by large differences in shot positions, and 70 of the 153 coordinate plots (46%) showed differences of 5mm or more. The Pareto dominant plans dominated other nearby plans. Pareto dominant plans represent different dosimetric tradeoffs and can be systematically calculated using genetic algorithms. Automatic identification of non-intuitive planning strategies may be feasible with these methods.

Key words: Gamma Knife; Radiosurgery; Pareto; Genetic algorithm.

Introduction

Recent advances in Gamma Knife software offer an abundance of intriguing options to construct conformal treatment plans (1, 2). Although these options are used to search for the best possible plan, such searches can be overwhelming due to the sheer number of choices. Compounding the problem is the absence of definitive methods to assess whether a particular plan is optimal, despite the need for such methods to guide treatment planning. Without a way to navigate the myriad choices of planning parameters and to assess individual plans, it is not likely that the impressive capabilities of the Gamma Knife software can be fully realized.

One approach to these problems is to guide the planning process with a cost function, in which a single number (the cost) is calculated to assess the value of a given plan. An example is the Paddick Index (PI), defined as the percentage of tumor within the treatment isodose volume multiplied by the percentage of treatment isodose volume within the tumor (3). These percentages are 100% for a perfect plan, so that the worth of a plan is measured by how close its PI is to 1. Another example is the cost function used by the new Gamma Knife software in

Corresponding author:
Cole A. Giller, MD, PhD, MBA
Phone: 706-721-3071
Fax: 706-721-8084
E-mail: cgiller@georgiahealth.edu

which a single weighted sum of tumor coverage, plan selectivity, gradient index and beam-on time is used to guide an inverse planning algorithm.

Any planning process is driven by at least two goals: to maximize the volume of tumor and minimize the volume of normal tissue within the treatment isodose volume. That these goals are conflicting is reflected by the common experience of reaching an impasse in planning in which covering more of the tumor cannot be achieved without also covering more normal tissue.

Unfortunately, using a cost function creates difficulties because the state of two different, conflicting planning goals cannot be fully measured by a single cost value. For example, the two schematic plans shown in Figure 1 emphasize these goals very differently, yet have the same PI. Such difficulties may have prompted a recent review to conclude that 'attempts to reduce conformation to a single index could lead to omission of essential information' (4).

Engineers also encounter settings in which conflicting goals must be optimized. For example, the design of bridges often requires compromises between expense and strength (5). The sophisticated methods developed for these problems include Pareto analysis (5, 6), in which a sequence of 'Pareto optimal' solutions are produced with the property that no such solution can be made to better satisfy one goal without degrading the performance of another. None of these solutions is an 'absolute best', and the final choice must be made using criteria other than the chosen goals. These solutions are analogous to the Gamma Knife plans mentioned earlier than cannot be made to cover more tumor without including more normal tissue.

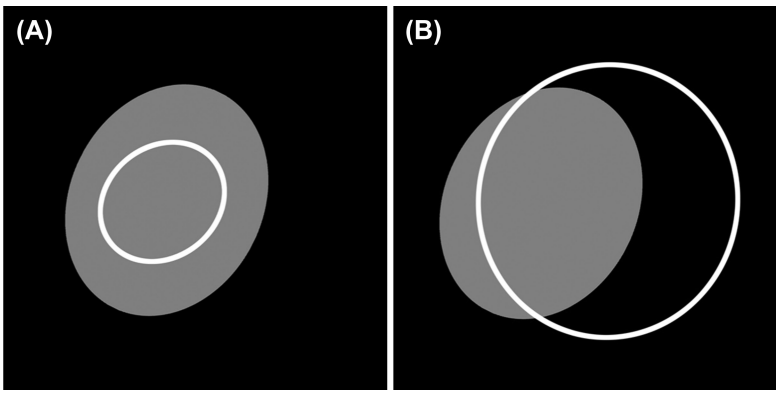

Figure 1: Schematic illustrating that strikingly different plans can have the same PI. (**A**) Schematic of tumor (shown in gray) containing treatment isodose volume (white circle). The percentage of tumor contained in the isodose volume is approximately 40%, and the percentage of the isodose volume contained in the tumor is 100%. The PI is therefore (0.4) (1.0) = 0.4. (**B**) The percentage of tumor contained in the isodose volume is approximately 80%, and the percentage of the isodose volume contained in the tumor is approximately 50%. The PI is therefore (.80) (.50) = 0.4.

Discovery of Pareto optimal solutions cannot be achieved by sheer calculation because the number of possible solutions is usually too large to test each solution individually. Efficient search algorithms have therefore been developed, including genetic algorithms in which the solutions are coded as if they were chromosomes and allowed to replicate, so that a selection process produces the 'fittest' (*i.e.,* most optimal) solutions (5, 7).

The goals of this manuscript can now be stated. The first goal is to apply Pareto analysis to the problem of finding optimal Gamma Knife plans, knowing that such plans must optimize two conflicting goals: covering more tumor and covering less normal tissue. The second goal is to demonstrate the feasibility of using genetic algorithms to produce a list of Pareto optimal Gamma Knife plans. The third goal is to suggest that each Pareto optimal plan can be viewed as a potentially non-obvious treatment strategy that can be easily completed to a final plan by the human radiosurgeon.

The scope of this work is limited to providing computer simulations suggesting that Pareto analysis may be a useful approach to Gamma Knife planning. The goal of providing a complete algorithmic package suitable for clinical use is laudable but too ambitious for this early treatment of these complex methods, and must be reserved for a future effort.

Material and Methods

Pareto Analysis

We now present the definitions of Pareto analysis (5) for Gamma Knife planning. In this discussion, a Gamma Knife plan will be said to cover a portion of tumor (respectively, cover a portion of normal tissue) when the treatment isodose volume of that plan covers that portion of tumor (respectively, that portion of normal tissue).

In general, Pareto analysis considers an optimization problem with two competing goals G1 and G2. A solution to the problem P1 is said to be *Pareto dominant* to a solution P2 if P1 satisfies both goals at least as well as P2 and satisfies at least one of the goals better than P2. In our case, a Gamma Knife plan P1 *Pareto dominates* a plan P2 if (1) P1 covers more tumor but not more normal tissue than P2 *or*, (2) P1 covers less normal tissue but not less tumor than P2.

A Gamma Knife plan P is *Pareto optimal* if no plan dominates P. In other words, there is no other plan that covers more tumor than P without covering more normal tissue, and there is no other plan that covers less normal tissue than P without also

covering less tumor. P is the type of plan mentioned earlier that cannot be improved upon in practice.

It is perhaps surprising that there are many Pareto optimal plans for each given tumor. However, it is common experience that each choice of planning parameters (number of shots, weights, collimator sizes, *etc.*) leads to a plan that cannot be further optimized, *i.e.,* to a Pareto optimal plan. Because there are a large number of such planning choices, there are an equally large number of different Pareto optimal plans. Note that because each such plan arises from different planning parameters, each Pareto optimal plan can be viewed as representing a different planning strategy.

If a treatment plan is allowed to have a very large number of shots, then it is usually possible to construct a virtually perfect plan that includes all of the tumor and only the tumor within its treatment isodose volume. Such a plan will be Pareto optimal, but may not be unique because different configurations of large numbers of shots might also produce perfect plans. In practice, however, plans are limited to a small number of shots, a perfect plan may not exist, and the set of Pareto optimal plans represents a meaningful collection of planning strategies. For this reason, the arguments in this manuscript will assume that the number of shots is fixed at a feasible size for routine practice.

We will measure the coverage of the tumor by the percentage of tumor contained within the treatment isodose volume, and will consider the maximization of that measurement as the first of our conflicting goals. We will measure the coverage of the normal tissue, however, by the actual volume of normal tissue contained within the treatment isodose volume (in mm^3) to reflect clinical needs. The minimization of this measurement will be the second of our conflicting goals. We will write Tumor(P) for the percentage of tumor covered by P, and we will write Normal(P) for the volume of normal tissue covered by P. In Pareto analysis, these are called the *multiobjective functions.*

If each plan P is graphed according to its multiobjective functions, with Tumor(P) vs. Normal(P), the Pareto optimal plans often form a convex curve (Figure 2). No plan can exist to the left of the curve, because such a plan would cover more tumor and less volume than some plan P on the curve, and so would dominate a non-dominatable P. In addition, all of the non-Pareto optimal plans would fall to the right of the curve. For these reasons, the described curve is often called the *Pareto front*.

It is instructive to consider plan A and plan B in Figure 2. Because of their positions on the graph, B covers more tumor and more normal tissue than. Thus B is 'better' than A because B covers more tumor, but A is 'better' than B because A covers less normal tissue. Neither of these Pareto optimal plans can therefore said to be 'better' than the other, nor is there a plan that is 'better' than all others.

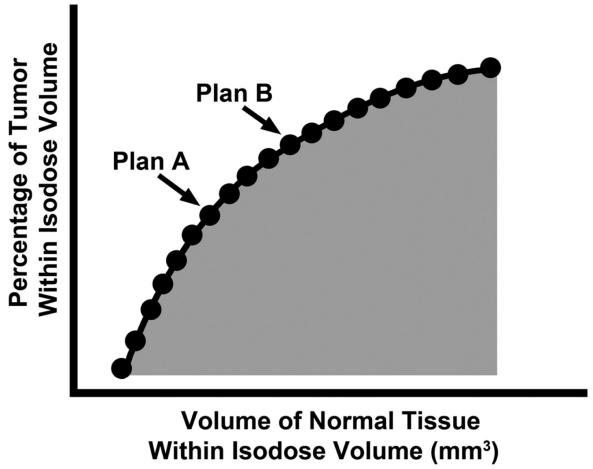

Figure 2: Schematic graph of Pareto optimal plans. Each dot represents a plan. For each plan P, the x-coordinate of the dot corresponding to P is the volume of normal tissue covered by P (*i.e.,* Normal(P)), and the y-coordinate of the dot is the percentage of tumor covered by P (*i.e.,* Tumor(P)). Because plan **B** lies above and to the right of plan **A**, **B** covers more tumor and more normal tissue than **A**. **A** is thus 'better' for normal tissue while **B** is 'better' for tumor. The curve produced by the Pareto optimal plans is often convex, as shown here, and is called the *Pareto front.* No plan can lie to the left of the curve (see text).

Calculation of Pareto Optimal Plans with Genetic Algorithms

In theory, Pareto optimal plans could be identified by testing each possible plan for Pareto dominance over all other plans, *i.e.,* by calculation of Tumor(P) and Normal(P) for each possible collection of Gamma Knife parameters and picking the Pareto dominant plans by comparing the various values. This approach is not possible, however, because of the number of possible plans. For example, even if the x, y and z coordinates are constrained to take only the 9 values between −2 cm and 2 cm in 5 mm increments, the number of possible plans using 3 shots is more than 380 million.

Pareto optimal plans must therefore be identified by efficient search algorithms. One such method is that of genetic algorithms, in which the plans are coded as if they were chromosomes (5, 7). For example, a plan using a shot with coordinates (x_1, y_1, z_1) and weight w_1 would be considered to have a 'gene' composed of the sequence x_1 y_1 z_1 w_1 along a 'chromosome' (Figure 3). The various chromosomes are then allowed to replicate with crossovers and mutations. A new collection of 'fittest' chromosomes is then formed by selecting the chromosomes from the resulting population which best optimize the multiobjective functions (*i.e.,* by selecting the plans that cover more tumor and less normal tissue). This process is repeated

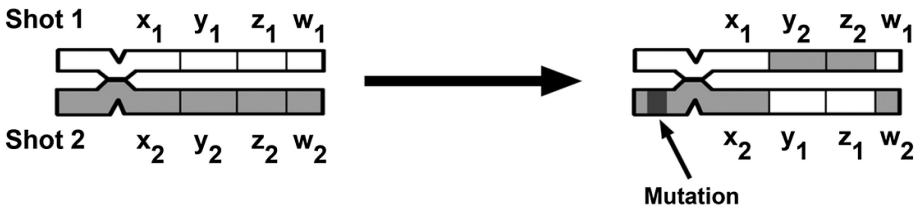

Figure 3: Diagram showing how Gamma Knife shot parameters can be coded as chromosomes by genetic optimization algorithms. On the left side of the Figure, each of two shots are considered to be portions of a chromosome with the spatial coordinates x, y, and z and the weight w serving as 'genes'. To generate the next plan to evaluate, the chromosome is allowed to 'replicate' with crossover and mutation. In this diagram, the y and z coordinates have been interchanged as part of the replication process to generate new shots. Other changes in the individual genes are programmed to occur at a chosen random 'mutation' rate, as indicated here schematically. A collection of new plans are produced by using the new shots generated when pairs of 'chromosomes' are allowed to replicated. Only the new plans that best optimize the multiobjective functions Tumor and Normal are chosen to replicate again, and the process repeats until optimization is achieved.

until the multiobjective functions cannot be optimized further. Genetic algorithms have been constructed to specifically find Pareto optimal solutions, and have been shown to rapidly converge under a variety of conditions (5).

The genetic algorithm chosen for this work is that used by the Multiobjective Genetic Algorithm Solver component of Matlab (Matlab, The MathWorks, Natick, Massachusetts). This algorithm identifies plans on the Pareto front by calculating the non-dominated plans of each generation using a highly optimized routine corresponding to the NSGA-II algorithm in the monograph by Deb (5). To find the Pareto optimal plans using n shots, the number of variables was set at 3n if the shot weights were held constant at 1, and set at 4n otherwise. The spatial variables were allowed to range between −15 and 15 mm, whereas the variables for weight were allowed to range between 0 and 1 (in most cases weights were not held constant). The output of the algorithm was a list of Pareto optimal plans, each consisting of the specific 4n coordinates and accompanied by their corresponding multiobjective functions Tumor(P) and Normal(P).

The Matlab genetic algorithm allows the choice of various parameters. An example is the number of chromosomes comprising each test population (the 'population size'), and it is generally accepted that an optimal population size should be high enough to cover the Pareto front and yet low enough to be computationally tractable. A review by Haupt *et al.* (7) showed that the optimal size determined by several studies using a variety of objective functions range between 20 and 100. Accordingly, we chose a population size of 60, the midpoint of this range.

Other parameters determine the methods of creating mutations, crossover strategies, and of choosing the initial distribution of chromosomes. The choices made here were those used most in common practice (5, 7): mutations were created by an 'adaptive feasible' algorithm that randomly generated mutations; a crossover strategy in which crossover sites were determined by the choice of a random binary vector; and the initial distribution of chromosomes was random, subject to the constraint that the shots were contained in the defined stereotactic space.

Prior to the 17 runs reported here, pilot data consisting of several runs using two to four shots were obtained for each of the tumor configurations. Because the Pareto fronts were similar in each case, each of the 17 reported scenarios were represented by a single run.

In general, a multiobjective genetic algorithm is adjusted to stop when the change in the objective functions between successive generations is small, because further calculation will not produce appreciably better solutions. The Matlab algorithm bases the calculation of this change on the 'crowding distance', defined as half of the perimeter of a rectangle centered at the given solutions with the two nearest neighboring solutions as vertices (5). The change is then calculated as a weighted average of these distances between successive generations, using both objective functions. For the data presented here, the algorithm halted when this change was less than 0.1 (the 'tolerance level'). This value was chosen both because it is small compared to the values taken by one of the objective functions (Normal(P)), and because pilot data based on sample runs showed that the Pareto fronts produced using a tolerance of 0.1 did not differ from those produced using smaller tolerances.

Gamma Knife Simulator

The genetic algorithm reduced the number of plans to be tested from many millions to thousands, but there were still too many plans to be entered by hand into the Gamma Knife software. An automatic calculation of Gamma Knife plans was therefore required, but because access to the Leksell Gamma Knife system was not available, a Gamma Knife 'simulator' was written using the Matlab software that could automatically be called from the Matlab software.

The input to the Gamma Knife simulator is a series of shots representing a plan P, each shot consisting of a vector (x, y, z, w, c) where x, y and z are spatial coordinates, w is the shot weight, and c denotes the collimator size (4, 8, 14 or 18 mm). The simulator then calculates the dose matrix within a $4 \times 4 \times 4\,cm^3$ cube, and displays the desired isodose lines using slices of 1 mm thickness (Figure 4). Alternatively, the software can be modified to return the values of Tumor(P) and Normal(P) to the genetic algorithm. The effects of beam attenuation were not included, and this omission does not effect the testing of the feasibility of Pareto analysis.

The simulation software allows the user to create a phantom 'tumor' by using the cursor to draw a polygon on each slice (Figure 4). The polygons are interpreted as a single tumor that can be used to calculate Tumor(P) and Normal(P) for any plan P. Tumors can be saved and loaded as needed.

The configuration of shot sources used most often consisted of 98 sources arranged symmetrically along three circles placed at 30, 50 and 70 degrees above horizontal and lying within a sphere of radius 40 cm. A full complement of 201 sources was not used in order to minimize computation time. Dose matrix calculation was performed by summing dose densities emanating from each source as described in the Gamma Knife software manuals (8).

Phantom Tumors and Test Runs

Three phantom tumors were used to test feasibility. A 'simple' tumor was designed to approximate a sphere; a 'bowtie' tumor was designed with two lobes; and a 'round' tumor was designed with eccentricity in one direction inferiorly and eccentricity in a perpendicular direction superiorly (Figure 5).

A total of 17 runs were performed. The 50% isodose volume was used in all calculations. Three of the runs used the simple tumor, 7 used the bowtie tumor and 7 used the round tumor.

Shot combinations were chosen to best reflect planning strategies seen in practice. For example, plans for the simple tumor were chosen that used various numbers of shots of similar size (4 mm) to the tumor itself. Plans for the bowtie tumor were chosen with different numbers of shots of a single size to test whether this strategy would provide coverage of both lobes of the tumor, and then with shots of different sizes to explore whether plans taking advantage of the subsequent renormalization would be chosen by the genetic algorithm. Larger shots were used for the round tumor to fill the larger volume of tumor. The shot weights were constrained to be 1 in the initial nine runs to gain experience with the Pareto algorithm, and thereafter were allowed to range freely between 0.1 and 1.

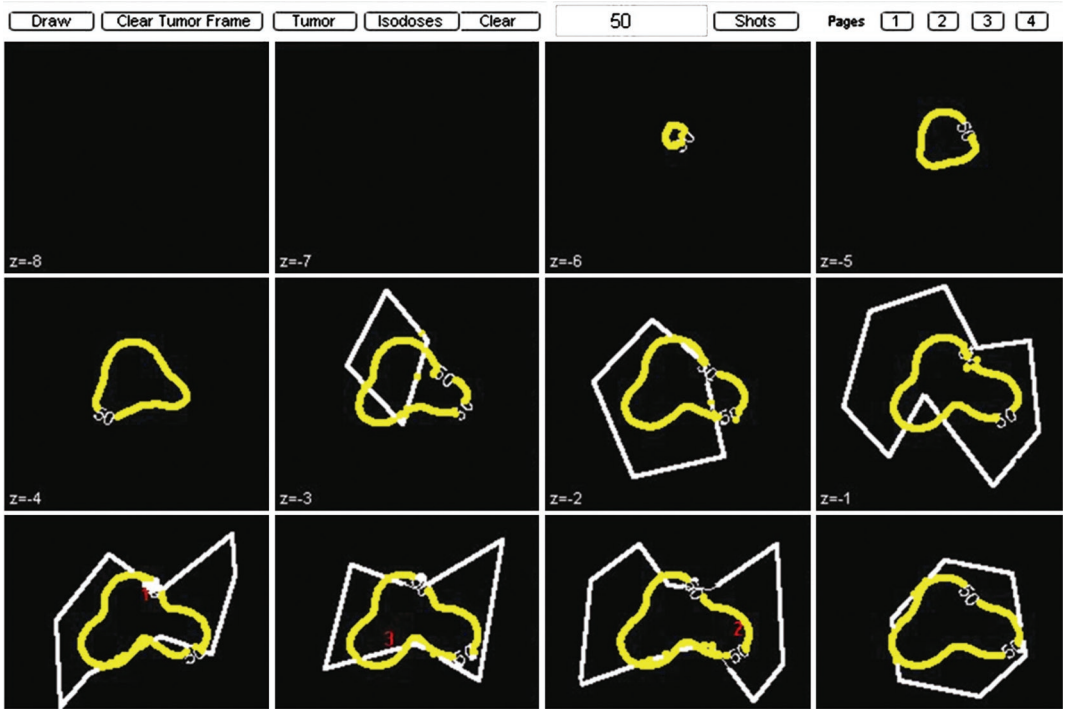

Figure 4: User interface for the Gamma Knife Simulator. Each panel represents a 1 mm slice, with four available pages covering a $4 \times 4 \times 4\,cm^3$ volume. The location of the shots is indicated by the red numerals, and the chosen isodose in this case (50%) is shown in yellow. The 'Draw' option allows the user to interactively create polygons in each panel (shown here in white) that determine a virtual 'tumor'. Shots are placed using a separate menu that is not shown.

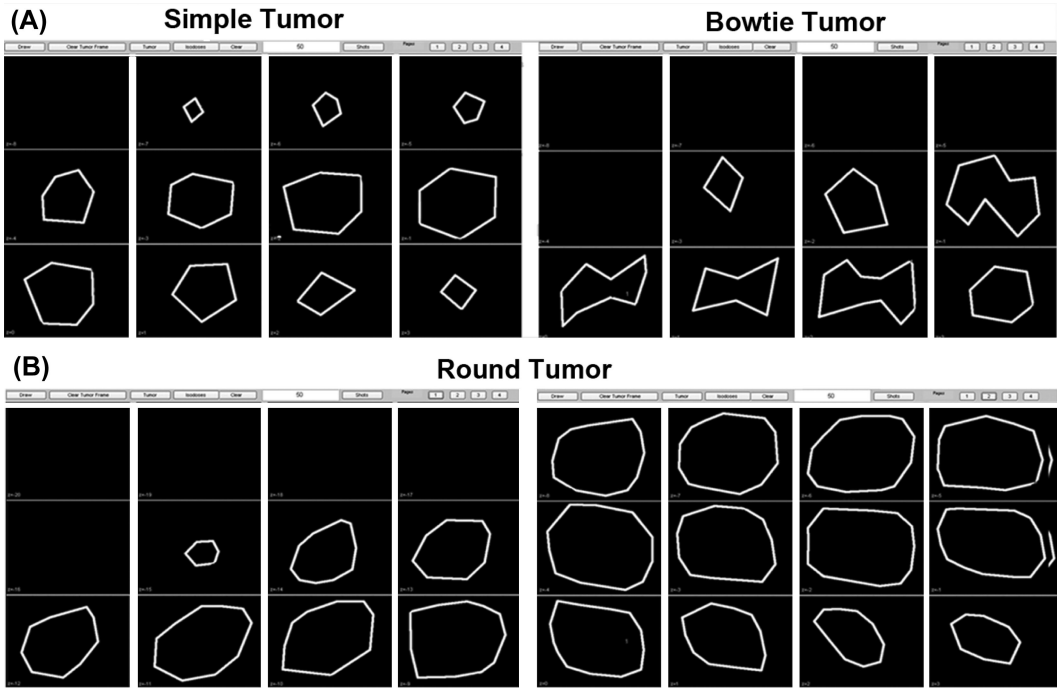

Figure 5: The three virtual tumors used for analysis are shown. (**A**) The shape of the 'simple' tumor approximates a sphere (left). The 'bowtie' tumor has an extension to the left and an extension to the right. (**B**) The round tumor is larger and requires two panels to display. The inferior pole (left) has eccentricity in one direction (viewer's right), while the superior pole (right) has eccentricity in the opposite direction.

The number of shots used and the allowed weights are summarized in Table I.

Table I
Summary of run parameters.

		Collimator[1]			
Run	Tumor	4 mm	8 mm	14 mm	Weights[2]
1	Simple	2			1
2	Simple	3			1
3	Simple	4			1
4	Bowtie		2		1
5	Bowtie		2		1
6	Bowtie	3			1
7	Bowtie	2	1		1
8	Bowtie	1	1		1
9	Bowtie	4			1
10	Bowtie	2	1		0.1 to 1
11	Round		2		0.1 to 1
12	Round		3		0.1 to 1
13	Round		3		0.1 to 1
14	Round		4		0.1 to 1
15	Round		2	1	0.1 to 1
16	Round		3	1	0.1 to 1
17	Round		4	1	0.1 to 1

[1]Numbers indicate number of shots.

[2]Weights were either fixed at 1 or allowed to range between 0.1 and 1.

Examination of Data

Each run produced between 40 and 80 Pareto optimal plans together with their values of the objective functions Tumor(P) and Normal(P). Figure 6A follows the usual custom of presenting Pareto data by plotting the values of one objective function against the other, in this case showing plans using four 8 mm shots to cover the round tumor. Normal(P) is plotted on the abscissa so that the shape of the resulting Pareto front best resembles that shown in other studies (5-7).

All of the Pareto fronts produced in this study were convex, as predicted from their representation as approximations of the true Pareto fronts.

It is of interest to examine how the individual treatment parameters of shot position and weight varied among the Pareto optimal plans produced by a given run. To this end, each plan P was assigned a unique plan number consisting of its rank when the list of plans was ordered by Normal(P). In other words, the plan number of the plan with the smallest value of Normal(P) was 1, the plan number of the plan with the next highest value of Normal(P) was designated as 2, and so on. The individual values of the x, y, z, coordinates and w values were then plotted against the plan number to assess the differences of these coordinates among the various plans.

Figure 6B is an example of such a graph. Note that because the plans are ordered according to their Normal(P) values, Figure 6B can be directly compared with Figure 6A.

Inspection of Figure 6B shows that the plan parameters change abruptly between plan 29 and plan 30, despite only a minimal change in the Tumor(P) and Normal(P) values

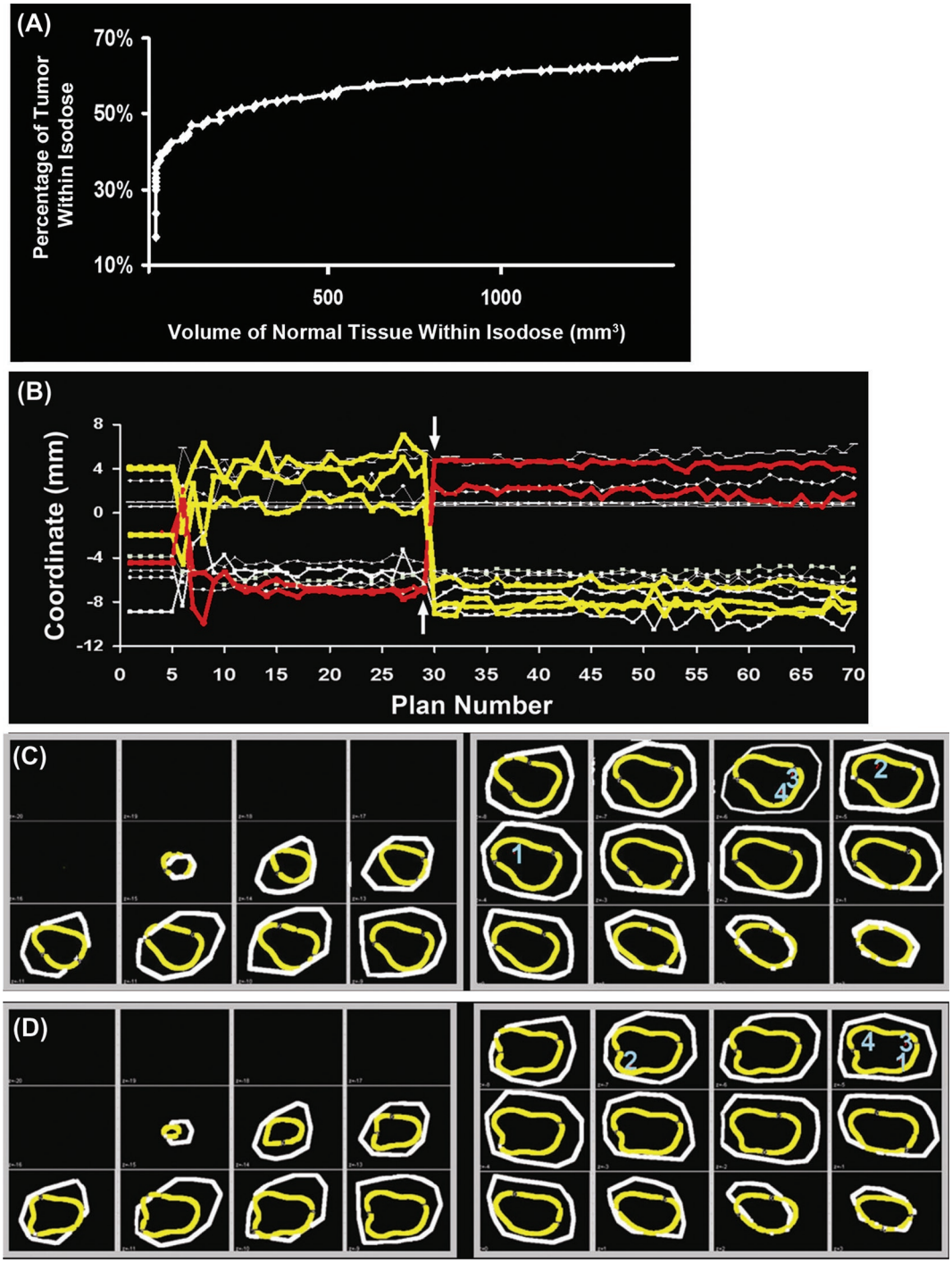

Figure 6: Pareto calculations for plan covering round tumor using four 8 mm shots. For reference, these shots will be called S_1, S_2, S_3 and S_4. (**A**) Graph of Tumor(P) vs. Normal(P) showing Pareto front as an approximation of a convex curve. There are 70 Pareto optimal plans. (**B**) Graph of the 12 spatial coordinates and 4 weights of the 4 shots vs. plan number. Color and line thickness have been added for emphasis. Three of the coordinates (the y-coordinates of S_1 and S_2 and the x-coordinate of a S_3) are shown in yellow and suddenly decrease between plan 29 and plan 30; two of the coordinates (the y-coordinate of S_3 and the x-coordinate of S_1) are shown in yellow and suddenly increase at the same point. This transition denotes a change in planning strategy. (**C**) The 50% isodose curves (yellow) and the tumor (white) are shown for plan 29. Blue numbers indicate the centers of the shots. Note that the isodose curves are eccentric to the left, matching the tumor eccentricity superiorly but not inferiorly. (**D**) The 50% isodose curves (yellow) and the tumor (white) are shown for plan 30. Note that the shot position has shifted significantly and that the isodose curves are equally eccentric superiorly and inferiorly. Vertical arrows indicate positions of plan 29 and plan 30.

(compare Figure 6A). Specifically, the y-coordinates of two of the shots and the x-coordinates of one of the shots for plan 30 are markedly smaller than those for plan 29, and the y-coordinate of one shot and the x-coordinate of one shot for plan 30 are markedly larger than those for plan 20. These changes are reflected by the rapid changes in the lines corresponding to these coordinates in Figure 6B, shown in yellow and indicated by arrows.

These changes can be viewed as indicating changes in planning strategy. For example, Figure 6C shows that plan 29 uses the strategy of placing shots to create isodose lines that are more conformal to the eccentricity of the tumor superiorly (right panel) than inferiorly (left panel). On the other hand, plan 30 uses the strategy of placing shots to optimize conformality at the bot portions of this eccentric tumor. This example suggests that large changes in these types of graphs can be viewed as indicating significant changes in planning strategy.

Results

To facilitate identification of these transitions, the separate shot coordinates were plotted on a single graph as the ordinate, with the plan number as the abscissa (Figure 6). Some of the coordinates changed very little, while others showed large variations that produced a large number of transitions. Individual plans at the transitions were examined with the Gamma Knife simulator to demonstrate the associated planning strategies.

A recognizable Pareto front was obtained from all 17 runs. The overall mean number of shots used in each run was 3.0 ± 0.8 (sd), and the mean number of shots used for the simple, bowtie and round tumor was 3.0 ± 1.0, 2.7 ± 0.8, and 3.3 ± 0.8, respectively. The overall mean number of identified Pareto optimal plans was 59 ± 17, and the mean number of plans for the simple, bowtie and round tumor was 62 ± 20, 54 ± 16 and 64 ± 18, respectively.

The volume of normal tissue covered by the Pareto optimal plans taken as a group ranged between 0 and 7579 mm^3, and the percentage of the tumor covered by the Pareto optimal plans taken as a group ranged between 0.3 and 93%. The range of the volume of normal tissue covered (*i.e.,* maximum value – minimum value) over the Pareto optimal plans ranged between 57 and 7574 mm^3 (median 1735 mm^3, mean 2133 ± 1933 mm^3 (sd)). The range of percentage coverage of the tumor (*i.e.,* maximum value – minimum value) ranged between 16 and 80% (median 42%, mean 41 ± 15%).

To assess the presence of coordinate transitions, the variation of the coordinates of the Pareto optimal plans was examined. For runs using n shots, there were 3n possible coordinates, and the range (maximum-minimum) of each of these 3n values (taken over the Pareto optimal plans generated by that run) was computed for each run. The 17 runs used 51 shots and so $3 \times 51 = 153$ coordinate ranges were examined.

Of these 153 coordinate ranges, 70 (46%) were greater than or equal to 5 mm (5 mm was felt to be a significant change in coordinates when planning, and so was chosen as a threshold to examine the various coordinate ranges). Of the 27 coordinate ranges used for by the runs for the simple tumor, 8 (30%) were greater than 5 mm. Of the 57 coordinate ranges used for by the runs for the bowtie tumor, 14 (25%) were greater than 5 mm. Of the 69 coordinate ranges used for by the runs for the round tumor, 48 (70%) were greater than 5 mm.

Of the 51 ranges for the x-coordinate (respectively, y-coordinate and z-coordinate), there 35 (respectively, 29 and 6) were greater than 5 mm. The percentage of x-coordinates and the percentage of y-coordinates greater than 5 mm was significantly greater than the percentage of z-coordinates greater than 5 mm, but there was no significant difference between the percentage of x-coordinates greater than 5 mm and the percentage of y-coordinates greater than 5 mm (χ^2, $\alpha = .05$).

The software used here required approximately 10 seconds for each dose distribution calculation, and assumed the use of only 98 sources. However, the Gamma Knife software is highly optimized and is much faster, calculating dose distributions such as shown here virtually instantaneously. Assuming that plans using 201 sources (as for the Model C) will require $201/98 = 2.05$ as much time as those using 98 sources, and assuming a dose distribution time of 0.25 seconds, the genetic algorithm used here (typically using 1000 to 5000 such calculations) would require between nine and 46 minutes if performed with the true Gamma Knife software.

Example One

In this run, four 8 mm shots were used to find Pareto optimal plans for the round tumor, with shot weights ranging between 0 and 1. Seventy Pareto optimal plans produced a convex Pareto front (Figure 6). A plot of the coordinates shows a clear transition occurring between Plan 29 and Plan 30, as well as smaller transitions between Plan 5 and Plan 29 (Figure 6).

Examination of the 50% isodose lines for Plan 29 and Plan 30 showed a shift in planning strategy as predicted by the coordinate transitions (Figure 6). In Plan 29, the shots are positioned to produce isodose curves that are oblique to the left. This obliquity matches that of the tumor superiorly, but is perpendicular to that of the tumor inferiorly; the plan therefore covers more tumor superiorly than inferiorly. In Plan 30, the shot positions have shifted so that the isodose curves have very little obliquity, so that the tumor coverage is more

evenly distributed between the superior and inferior aspects of the tumor. The multiobjective functions of the two plans were virtually identical (96 vs. 105 mm^3 and 45 vs. 47%), although the multiobjective functions diverge for plans farther away from the transition point. It is important to note that these plans are Pareto optimal – neither is strictly better than the other at covering both more tumor and less normal tissue – and the decision of which to use would be made on separate clinical and anatomic grounds.

Example Two

In this run, one 8 mm and two 4 mm shots were used to find Pareto optimal plans for the bowtie tumor, with shot weights ranging between 0 and 1. Seventy-two Pareto optimal plans produced a Pareto front (Figure 7). A plot of the coordinates shows high variability of the coordinates producing many transitions and many potential planning strategies.

Six such plans are shown in Figure 7, together with their position along the plan axis. The shots are clustered together in Plan 1, producing collapsed isodose curves. Note that Pareto optimality is reflected by the adjacency of the isodose curves to the tumor boundary so that further enlargement cannot be achieved without coverage of more normal tissue. Plan 13 demonstrates the strategy of filling one arm of the bowtie shape by spreading the shots apart. Plan 15 uses a 4 mm shot to fill an arm of the bowtie shape, while adjusting the shots to cover as much of the superior and inferior tumor poles as possible. Plan 27 keeps the 8 mm shot in a central position, using the two 4 mm shots to fill each arm of the bowtie shape. Note that the increase in tumor coverage is achieved at the cost of more normal tissue covered inferiorly. Plan 32 is similar to Plan 27, but the shots have been shifted to cover more of the superior pole while still covering the arms of the bowtie shape. A different strategy is represented by Plan 51, in which the 8 mm shot and one of the 4 mm shots create a widening of the isodose curve centered to one side of the bowtie shape, while the other 4 mm shot is used to cover as much as possible of the other side. It is again important to note that these plans are all Pareto optimal – those that cover more tumor than others also cover more normal tissue, and the choice of the best plan must be made on clinical grounds alone.

Example Three

In this run, three 4 mm shots were used to find Pareto plans for the simple tumor, with shot weights ranging between 0 and 1. Again, a distinct Pareto front was produced (Figure 8). Plan 20 was chosen arbitrarily to demonstrate Pareto optimality. Each coordinate of each shot used by Plan 20 was individually increased and then decreased by 1 mm, 2 mm and 3 mm, and the multiobjective functions calculated for the resulting 54 (6 variations for each of the 9 coordinates) plans. Each plan was plotted according to its multiobjective function, using different colors for different amounts of variation (Figure 8). Most of the plotted points lie beneath the curve; only two lie above, and these two are lie very close to the curve itself. This demonstrates that the calculated curve is a close approximation to the true Pareto front (at least for Plan 20), as the points do not venture into the region of solutions that would dominate the calculated Pareto optimal plan.

Discussion and Conclusions

This manuscript presents simulation data suggesting that Pareto analysis may be feasible for Gamma Knife planning. Because Pareto analysis for Gamma Knife radiosurgery is largely unexplored, production of a complete, clinical package is beyond the scope of this first effort, and this work has therefore been limited to computer simulations. The ultimate goal will be to incorporate these ideas into actual radiosurgical software.

The ideas proposed in this work represent an unconventional view of Gamma Knife planning in at least three ways. First, instead of searching for a plan that best optimizes a single-valued cost function, we instead produce a list of Pareto optimal plans that vary in their ability to simultaneously cover the tumor and exclude normal tissue. Identification of Pareto optimal plans may be more clinically relevant than finding plans that optimize a cost function, because any plan that optimizes a cost function without covering the entire tumor (as is likely for complex tumors) is either itself Pareto optimal or dominated by a Pareto optimal plan. In either case, this plan cannot simultaneously optimize the coverage of both tumor and normal tissue better than the other Pareto optimal plans, and is therefore not better than all other plans. The best plan may therefore be one chosen from the list of Pareto optimal plans on clinical grounds.

The second unconventional viewpoint presented here is to view each Pareto plan as a treatment strategy, and to seek a collection of treatment strategies rather than a collection of fully completed plans. That each Pareto optimal plan can be viewed as a strategy is demonstrated by the observation that small perturbations of the planning parameters (*e.g.,* shot locations) of a Pareto optimal plan result in plans that are less optimal (Figure 8), showing that each Pareto optimal plan is unique among its near neighbors. The proposal discussed here is therefore to use Pareto analysis to produce a list of non-intuitive strategies (Pareto optimal plans) that might otherwise be difficult to identify, choose the strategy that best satisfies clinical demands, and then complete the associated Pareto optimal plan to a usable, complete plan. Such

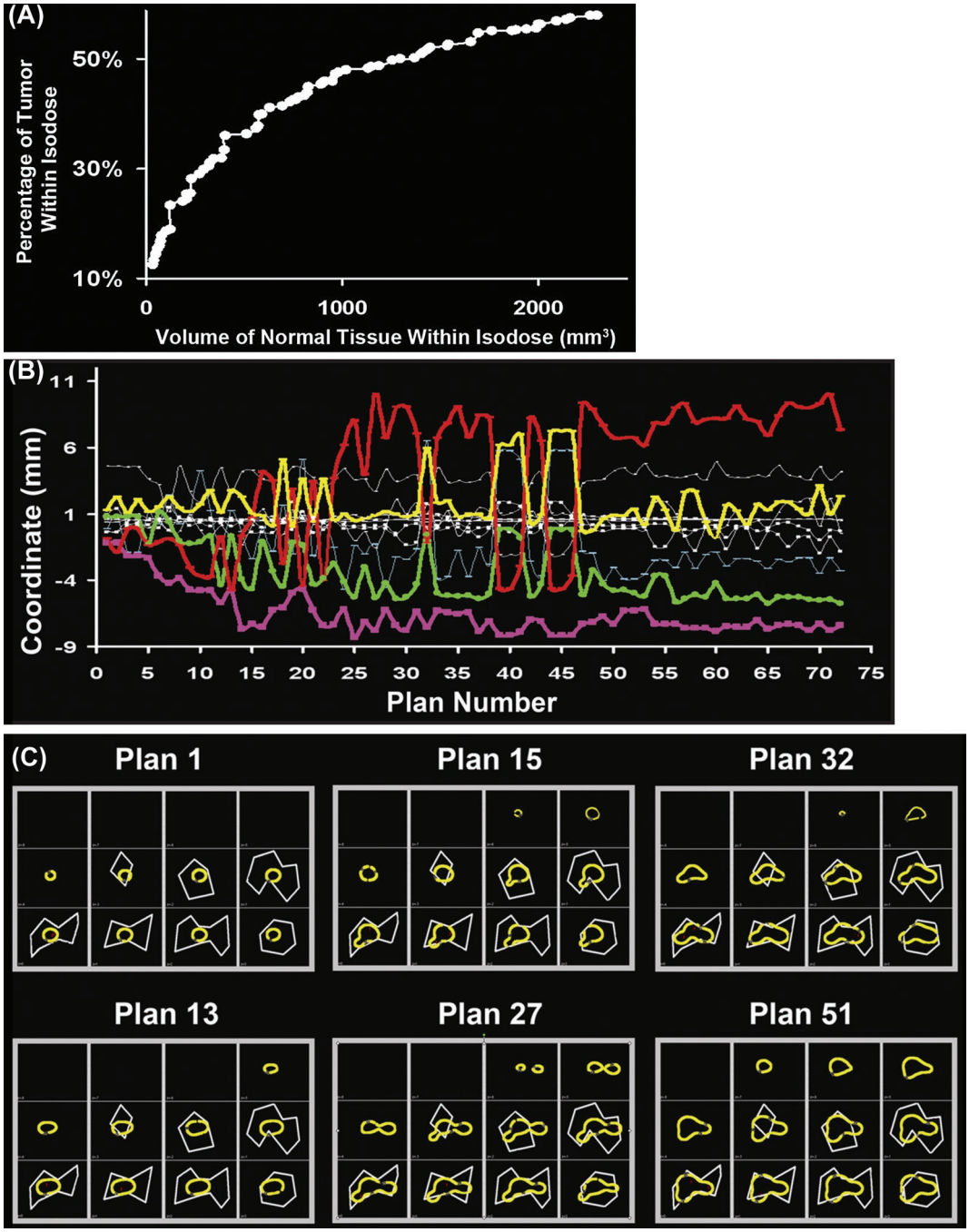

Figure 7: Pareto calculations for plan covering bowtie tumor using one 8 mm and two 4 mm shots. (**A**) Graph of Tumor(P) vs. Normal(P) showing Pareto front as an approximation of a convex curve. There are 72 Pareto optimal plans. (**B**) Graph of the 9 spatial coordinates and 3 weights of the 3 shots vs. plan number. Color and line thickness have been added for emphasis. Note the frequent variation of coordinates indicating multiple planning strategies. (**C**) Isodose curves of 6 representative plans from transition points indicated by graph in (**B**). Each plan represents a different planning strategy (see text).

completion can be easily achieved by a human operator by, for example, adding a suitably large number of small shots. One might conjecture that automatically producing complete Gamma Knife plans for complex tumors is not tractable in clinical practice, whereas producing a list of Pareto optimal plans may represent an easier and perhaps more clinically relevant task.

The third unconventional viewpoint is the belief that a perfect plan is unattainable (at least for complex tumors), and that every plan harbors compromises between coverage of tumor and coverage of normal tissue. This belief is consistent with the common experience of arriving at a Gamma Knife plan that cannot be changed to cover more tumor without also covering more normal tissue, and the realization that

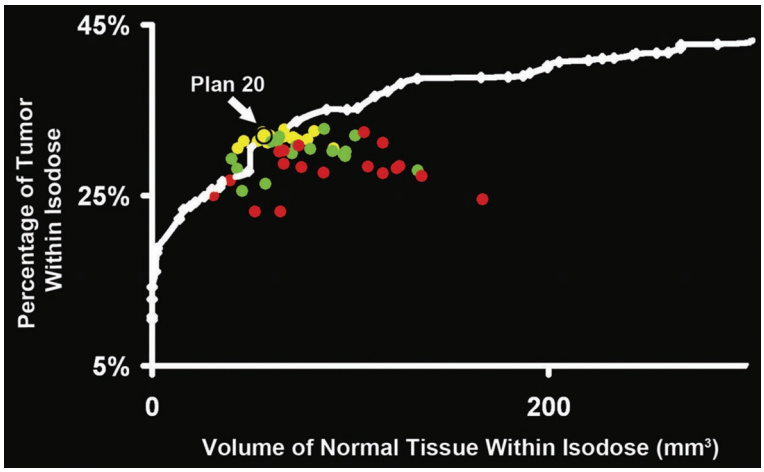

Figure 8: Pareto front from calculation for simple tumor using three 4 mm shots. Plan 20 was chosen arbitrarily to provide an example and is indicated by the black circle (its position is obscured by the overlying points). Each spatial coordinate of each shot of plan 20 was varied by ±1 mm, ±2 mm, and ±3 mm to produce plans that were graphed and shown here in yellow, green and red, respectively. The points cluster beneath the Pareto front or fill in its gaps to approximate the true Pareto front, providing evidence that the chosen plan is Pareto optimal (see text).

there are many such plans depending on the chosen planning strategy. Pareto analysis formalizes this common experience, emphasizing the reality that the different optimal plans must be chosen on clinical rather than mathematical grounds.

Because highly efficient algorithms already exist that produce conformal Gamma Knife plans, one might ask why an untested approach such as Pareto analysis should be considered. There are at least two answers. First, although many of the existing algorithms produce a single plan that best simultaneously maximizes coverage of tumor and minimizes coverage of normal tissue, the clinician is often more interested in trade-offs. For example, it may be advantageous to accept less tumor coverage if the resulting dose to highly sensitive critical structures is less; and conversely, it may be better to include non-eloquent tissue within the treatment isodose line if a higher dose to the tumor can be attained. Existing algorithms do not systematically provide the clinician with a list of such trade-offs for clinical consideration, whereas providing such a list is exactly the goal of Pareto analysis.

The second reason to consider Pareto analysis is because of the success of this method in other fields. Many problems faced by engineers parallel those of Gamma Knife planning: algorithms are available that 'lump together' the parameters such as cost and strength, but engineers are interested in choosing between the many possible tradeoffs (5). Furthermore, several studies have provided data supporting the utility of Pareto analysis for planning in radiation oncology (9-15). Pareto analysis is becoming a useful tool in an increasing number of applications, and deserves consideration for Gamma Knife planning as well.

The impact that Pareto analysis might have upon Gamma Knife planning is difficult to predict. On the one hand, such analysis might be expected to provide the radiosurgeon with a list of plans with varying degrees of tumor coverage, allowing choices to be made according to the clinical assessment of the tradeoffs between coverage of tumor and normal tissue. On the other hand, realistic radiosurgical planning mandates consideration of multiple parameters such as treatment time, gradient indices, plug patterns and the location of multiple isodose lines. Inclusion of these parameters in Pareto analysis is possible, but the computation requirements could be prohibitive. One can speculate, based on analysis of the examples shown here, that the true value of Pareto analysis might be to identify planning strategies that are not otherwise obvious. A final plan could then be constructed by a human operator, armed with these new strategies.

Although Pareto analysis has received little attention for Gamma Knife planning, a wide variety of methods have been explored for this purpose. Dean *et al.* (16) used scaling factors within an optimization routine to model the tradeoffs between dose delivery to tumor and normal tissue. Tradeoffs were explored with evolutionary algorithm that optimized a single objective function rather than exploring tradeoffs through multiobjective optimization. Schlaefer *et al.* (17) explored tradeoffs by varying constraints of a single objective function optimization, and other authors have also employed a single objective function (18, 19). Luan *et al.* (20) described the use of 'dose painting' to minimize an objective function, calculating results with different constraints upon treatment time to address tradeoffs between dose and time. Hu *et al.* (21) introduced the concept of a moving isocenter ('tomosurgery') to construct an inverse planning algorithm that addresses two dimensional sub-problems. Heuristic algorithms to match the tumor anatomy have been developed (22, 23), and used in combination with minimization of single objective functions (24). Finally, the new Gamma Knife planning algorithm is an inverse planning method based on optimization of a single objective function, and has been recently explored by Shlesinger *et al.* (25). They concluded that even with this sophisticated algorithm, 'user-based optimization will be required to achieve an acceptable Gamma Knife dose plan'. Although some of these methods indirectly address planning tradeoffs through repetitive calculation or adjustment of constraints, none allow multiobjective optimization and none provide the radiosurgeon with a list of otherwise equivalent plans and strategies with various choices of tradeoffs as does Pareto analysis.

Although Pareto analysis has not been used extensively for Gamma Knife planning, Pareto methods have been proposed

as an optimization tool for inverse planning used in radiation oncology (14). Calculation of Pareto optimal plans and the use of multiobjective optimization has been proposed to optimize treatment planning (9, 14), optimize beam angle configurations in IMRT (10), assist planning for radiation therapy for pancreatic cancer (11), and compare treatment planning systems (13). Several authors have constructed computer interfaces designed to allow the user to interactively sample the Pareto front (9-11, 14), and a website is devoted to this topic (26). The search algorithms in general rely on the ability to formulate optimization for IMRT as a linear-programming problem, but some authors have used genetic evolutionary algorithms (12, 15). Unfortunately, linear methods are not available for Gamma Knife planning in which the delivery of clusters of beamlets as shots creates a non-linear environment.

A broad range of values of the multiobjective functions was observed, and the number of Pareto optimal solutions was relatively high (59 ± 17). Nevertheless, it is likely that some Pareto optimal plans were not detected by the algorithm, and that their corresponding planning strategies were not identified. Engineers refer to the range of Pareto optimal solutions detected by an algorithm as the *diversity*, and have developed methods to adjust the algorithmic parameters to maximize the diversity under many conditions (5). A direction for future work is to use these methods to maximize the number of identified Pareto optimal Gamma Knife plans.

Although the Pareto front identified by the search algorithms usually represents an approximation to the true Pareto front, the errors appeared to be quite small and acceptable for clinical use. Systematic variation of the shot positions of randomly selected Pareto optimal solutions produced plans that generally were dominated by the chosen plan (Figure 8), indicating that Pareto optimality had indeed been achieved in the majority of the runs.

The custom software used here requires approximately 10 seconds for each dose distribution calculation, and is therefore too slow for clinical implementation of the genetic algorithm which requires 1000 to 5000 such calculations. However, the true Gamma Knife software is highly optimized, and estimates given in the Results section suggest that Pareto solutions could be obtained within nine to 46 minutes. These times might be acceptable to some centers, and could be incorporated into their overall planning process. For other centers, preplanning techniques that allow planning calculations to be completed prior to the day of Gamma Knife treatment are available through the Gamma Knife software and as other ad hoc methods (27).

To facilitate computation, the Gamma Knife Simulator included only 98 sources. This produced isodose volumes that were more elongated in the z-direction than if a more standard collection of 201 sources had been used, and prevented the isodose volumes from being more conformal. Nevertheless, the various planning strategies could be identified from the Pareto optimal plans and the choice of 98 sources did not affect the question of feasibility.

This work represents a preliminary exploration (perhaps the first) of Pareto methods for Gamma Knife planning, and does not provide a complete software package useable for clinical practice. Although it is hoped that such a package will eventually be produced, this task is arguably too ambitious for a first effort in which a variety of conceptual and methodological issues must be addressed. As has been the case for other software packages, full development will require additional time, effort and refinement.

The Gamma Plans used here do not include complex shots available with the Perfexion device, and such inclusion is beyond the scope of this initial feasibility study. However, because complex shots are described by specific numerical parameters, Pareto analysis for such shots would be straightforward and could be addressed in future work.

The multiobjective functions used here (maximizing percentage of tumor covered and minimizing volume of normal tissue covered by the treatment isodose volume) were not the only possible choices; any measurements of coverage would have produced analogous Pareto optimal plans. For example, sample calculations show that maximizing the percentage of tumor covered by the treatment isodose volume and maximizing the percentage of the treatment isodose volume covered

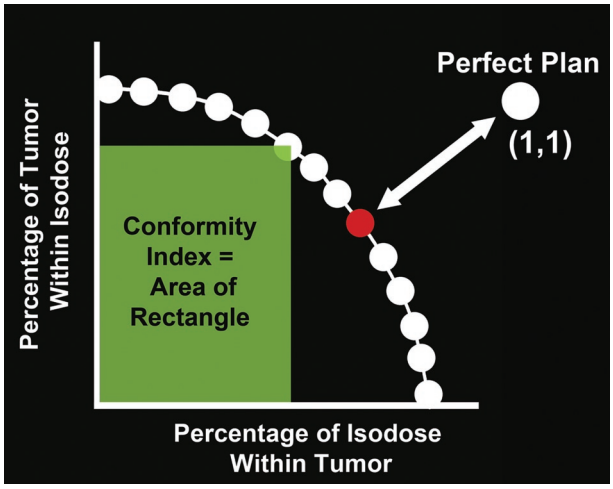

Figure 9: Schematic of Pareto front when the objective functions are the percentage of tumor within the isodose volume and the percentage of the isodose volume within the tumor. The PI of each Pareto optimal plan is the product of these two functions, and thus is the area of the rectangle with one vertex at the origin and another at the point representing the plan. The rectangle corresponding to the Pareto optimal plan yielding the maximum PI is shown in green. Note that this plan is not necessarily the plan that lies closest to the perfect plan (1, 1), shown here in red. See text.

by tumor (the two goals associated with the Paddick Index) produces recognizable Pareto fronts, permitting a similar analysis to the one presented here (Figure 9). Note that these fronts are mirror images of those shown before, because both of the variables are being maximized.

It is worth noting that the use of percentage coverage is not fully equivalent to volume coverage. To see this, let vP_1 be the volume of the treatment isodose volume for a plan P_1, let vP_2 be the volume of the treatment isodose volume for different plan P_2, let I_1 be the volume of the intersection of the treatment isodose volume of P_1 with tumor, and let I_2 be the volume of the intersection of the treatment isodose volume of P_2 with tumor. To say that Pareto analysis with the multiobjective functions chosen here (percentage of tumor covered, volume of normal tissue covered) is equivalent to analysis using percentage of tumor covered by the treatment isodose volume and percentage of isodose volume covered by the tumor is to say that whenever $I_1/vP_1 < I_2/vP_2$ then we must have $vP_1 - I_1 > vP_2 - I_2$. But it is straightforward to find both counterexamples ($vP_1 = 10$, $vP_2 = 20$, $I_1 = 5$ and $I_2 = 12$) and examples (same values except $I_2 = 18$). Because the use of different multiobjective functions produces a similar, but not necessarily equivalent set of Pareto optimal plans, the choice of such functions should depend upon the clinical goals of the optimization.

There is an interesting relationship between analysis using the PI and Pareto analysis. If the multiobjective functions mentioned above (percentage of tumor covered by isodose volume and percentage of isodose volume covered by tumor) are used for Pareto analysis, then the PI of any plan represented by a point on the Pareto front is the area of the rectangle constructed with that point and the origin as vertices (Figure 9). A perfect plan would be represented by the point (1, 1), and the plan with the most optimal PI (*i.e.,* with the largest PI) corresponds to the point P on the front which maximizes the area of the rectangle. However, P is not necessarily the point closest to the perfect plan (1, 1). For example, if the front is approximated by the curve $y = -ax^2 + b$ (where x = the percentage of isodose volume covered by tumor and y = the percentage of tumor covered by isodose volume), then it can be shown that the PI is maximal when $x = x_0 = (b/3a)^{1/2}$ and $y = y_0 = 2b/3$. The condition that (x_0, y_0) be closest to (1, 1) along the curve is equivalent to the condition that the vector from (x_0, y_0) to (1, 1) be perpendicular to the tangent to the curve at this point; but this condition can be shown to be a quadratic equation in the variable a. This means that for a given b, there can be at most two values of a that allow the point corresponding to the maximal PI to also be the point closest to (1, 1). In other words, in most cases, the plan that maximizes PI is not the plan that lies closest to the perfect plan. Because it is commonly assumed that a plan with maximal PI will lie closest to perfection, this is a surprising result. It is testimony to the difficulties arising when a single-valued cost function such as the PI is used to assess what is really a multidimensional problem; optimizing the weighting for a cost function is not necessarily equivalent to picking the best Gamma Knife plan.

It should also be noted that if a perfect plan exists, *i.e.,* if a plan exists corresponding to (1, 1) in the previous example, then each Pareto optimal plan must produce a treatment isodose volume that perfectly covers the tumor. The Pareto front would therefore be a single point representing a collection of different strategies producing the same (perfect) isodose volume, but containing no information regarding practical planning compromises. As noted before, however, such plans rarely exist for tractable numbers of shots.

Conclusion

This work attempts to show how Pareto analysis might be applied to Gamma Knife planning, using a simulation of radiosurgical calculations to demonstrate that a list of Pareto optimal plans can be automatically generated by a genetic algorithm. Such plans could provide the radiosurgeon with a choice of tradeoffs between dose delivery to tumor and normal tissue, and could suggest treatment strategies that might not otherwise be obvious. Further development of a clinically usable Pareto planning package may produce a useful addition to the planning armamentarium.

Conflict of Interest

The author certifies that regarding this paper, no actual or potential conflicts of interests exist; the work is original, has not been accepted for publication nor is concurrently under consideration elsewhere, and will not be published elsewhere without the permission of the Editor.

References

1. Giller, C. A., Fiedler, J. A., Gagnon, G. J., Paddick, I. *Radiosurgical Planning: Gamma Tricks and Cyber Picks.* Wiley-Blackwell, Hoboken, New Jersey (2009).
2. Lindquist, C., Paddick, I. The Leksell Gamma Knife Perfexion and comparisons with its predecessors. *Neurosurgery 62*(*Suppl. 2*), 721-732 (2008).
3. Paddick, I. A simple scoring ratio to index the conformity of radiosurgical treatment plans. Technical Note. *J Neurosurg 93*(*Suppl. 3*), 219-222 (2000).
4. Feuvret, L., Noel, G., Mazeron, J.-J., Bey, P. Conformity index: a review. *Int J Radiation Oncology Biol Phys 64*, 333-342 (2006).
5. Deb K. *Multi-Objective Optimization using Evolutionary Algorithms*. John Wiley and Sons, Chichester (2001).
6. Van Veldhuizen, D. A., Lamont, G. B. Multiobjective evolutionary algorithms: analyzing the state-of-the-art. *Evol Comput 8*, 125-147 (2000).
7. Haupt, R. L., Haupt, S. E. *Practical Genetic Algorithms*. John Wiley and Sons, Hoboken (2004).

8. Tseng, Y. J., Chang, H. H., Shiau, C. Y., Chung, W. Y., Pan, D. H., Chu, W. C. PC-based gamma knife radiosurgery dose calculation. *IEEE Eng Med Biol Mag 22*, 92-107 (2003).
9. Craft, D., Halabi, T., Shih, H. A., Bortfeld, T. An approach for practical multiobjective IMRT treatment planning. *Int J Radiation Oncology Biol Phys 69*, 1600-1607 (2007).
10. Craft, D., Monz, M. Simultaneous navigation of multiple Pareto surfaces, with an application to multicriteria IMRT planning with multiple beam angle configurations. *Med Phys 37*, 736-741 (2010).
11. Hong, T. S., Craft, D. L., Carlsson, F., Bortfeld, T. Multicriteria optimization in intensity- modulated radiation therapy treatment planning for locally advanced cancer of the pancreatic head. *Int J Radiation Oncology Biol Phys 72*, 1208-1214 (2008).
12. Lahanas, M., Baltas, D., Zamboglou, N. A hybrid evolutionary algorithm for multi- objective anatomy-based optimization in high-dose-rate brachytherapy. *Phys Med Biol 48*, 399-415 (2003).
13. Ottosson, R. O., Engstrom, P. E., Sjostrom, D., Behrens, C. F., Karlsson, A., Knoos, T., Ceberg, C. The feasibility of using Pareto fronts for comparison of treatment planning systems and delivery techniques. *Acta Oncologica 38*, 233-237 (2009).
14. Thieke, C., Kufer, K.-H., Monz, M., Scherrer, A., Alonso, F., Oelfke, U., Huber, P. E., Debus, J., Bortfeld, T. A new concept for interactive radiotherapy planning with multicriteria optimization: First clinical evaluation. *Radiotherapy and Oncology 85*, 292-298 (2007).
15. Yu, Y., Zhang, J. B., Cheng, G., Schell, M. C., Okunieff, P. Multiobjective optimization in radiotherapy: applications to stereotactic radiosurgery and prostate brachytherapy. *Artificial Intelligence in Medicine 19*, 39-51 (2000).
16. Dean, D., Zhang, P., Metzger, A. K., Sibata, C., Maciunas, R. J. Medial axis seeding of a guided evolutionary simulated annealing (GESA) algorithm for automated Gamma Knife radiosurgery treatment planning. In Niessen, W. J., Viergever, M. A. (Eds.), *Medical Image Computing and Computer-Assisted Intervention MICCAI 2011,* Springer-Verlag, Berlin, 2001, 441-448.
17. Schlaefer, A., Schweikard, A. Stepwise multi-criteria optimization for robotic radiosurgery. *Med Phys 35*, 2094-2013 (2008).
18. Ove, R., Popple, R. Sequential annealing-gradient Gamma-Knife radiosurgery optimization. *Phys Med Biol 48*, 2071-2080 (2003).
19. Luo, L., Shu, H., Yu, W., Yan, Y., Bao, X., Fu, Y. Optimizing computerized treatment planning for the gamma knife by source culling. *Int J Radiation Oncology Biol Phys 45*, 1339-1346 (1999).
20. Luan, S., Swanson, N., Chen, Z., Ma, L. Dynamic gamma knife radiosurgery. *Physics in Medicine and Biology 54*, 1579-1591 (2009).
21. Hu, X., Maciunas, R. J., Dean, D. A new Gamma Knife radiosurgery paradigm: tomosurgery. *Medical Physics 34*, 1743-1758 (2007).
22. Wu, Q. J., Bourland, J. D. Morphology-guided radiosurgery treatment planning and optimization for multiple isocenters. *Med Phys 26*, 2151-2160 (1999).
23. Lee, K. J., Barber, D. C., Walton, L. Automated gamma knife radiosurgery treatment planning with image registration, data-mining and Nelder-Mead simplex optimization. *Medical Physics 33*, 2532-2540 (2006).
24. Shepard, D. M., Chin, L. S., DiBiase, S. J., Naqvi, S. A, Lim, J., Ferris, M. C. Clinical implementation of an automated planning system for gamma knife radiosurgery. *Int J Radiation Oncology Biol Phys 56*, 1488-1494 (2003).
25. Schlesinger, D. J., Sayer, F. T., Yen, C. P., Sheehan, J. P. Leksell GammaPlan version 10.0 preview: performance of the new inverse treatment planning algorithm applied to Gamma Knife surgery for pituitary adenoma. *J Neurosurg 113*(*Suppl*), 144-148 (2010).
26. MIRA. www.project-mira.net. Accessed June 9, 2010.
27. Giller, C. A., Fiedler, J. A. Virtual framing: the feasibility of frameless radiosurgical planning for the Gamma Knife. *J Neurosurg 109* (*Suppl*), 25-33 (2008).

Received: January 19, 2011; Revised: March 29, 2011; Accepted: April 15, 2011